Communication

Efficiency Bound of Radiative Wireless Power Transmission Using Practical Antennas

Joon-Hong Kim, Youngjoon Lim, and Sangwook Nam

***Abstract*— In this communication, we provide the efficiency bound of radiative wireless power transmission (WPT) for several types of practical receiving antennas. The optimal current distribution of the transmitting surface is analytically derived. In addition, the maximum bound of the power transfer efficiency (PTE) and the optimal shape of the base station current are found in terms of the transmitting area and the transfer distance. Examples applying the proposed theory to three types of practical mobile antennas are shown and the results are compared with those of previous reports, demonstrating significant differences. The results indicate that the optimum current distribution on the transmitting surface and the maximum efficiency of radiative WPT depend on the radiating field pattern of the mobile antenna. The results further show that microwave power transmission using a compact patch antenna can achieve high power transmission efficiency, especially in the Fresnel region.**

***Index Terms*— Efficiency bound, Fresnel zone, microwave power transmission (MPT), phase conjugation, power transfer efficiency (PTE), radiative near-field, radiative wireless power transmission (WPT), retro-directive array (RDA), time-reversal (TR).**

I. Introduction

Over the last few decades, wireless power transmission (WPT), which can charge the batteries of mobile devices without wires, has been developed to improve the convenience of mobile users. There are several WPT technologies, such as inductive coupling, resonant coupling, and microwave power transmission (MPT). Many recent studies on WPT have been conducted on inductive coupling and resonant coupling, which are based on the use of the near-field, or evanescent field. On the contrary, MPT, which is based on the propagating field, has not recently been studied as much, even though MPT can increase the operating range of WPT.

MPT was extensively researched in the 1960s using large array antennas [1]–[11]. Brown [1]–[3] conducted many pioneering experiments on MPT for high power applications. Glaser [4] proposed a future energy source in which a satellite that harvested solar power in space using huge array antennas transmitted the power to earth via a microwave beam. Goubau and Schwering [5], [6], Goubau [7], and Shinohara [8], [9] suggested a point-to-point reiterated microwave reply system using cylindrical waves and showed that a Gaussian beam was the approximately optimum transmitting source between two planar apertures, especially in the Fresnel zone, which is also known as the radiative near-field. Kay [10] and Borgiotti [11] also described the optimum field of a symmetric transmitting aperture for an ideal receiving aperture in the Fresnel region. In 1983, experiments on MPT applying the phased array technique were conducted in space using rockets in Japan [12]–[14]. Schlesak *et al.* [15] carried out experiments on a fuel-less airplane powered by a microwave beam using an array of parabolic antennas. The phase-controlled magnetron was designed and employed in airship MPT experiments by Shinohara and Matsumoto [16], Shinohara *et al.* [17], and Wang *et al.* [18]. In addition, studies on RF-dc rectifiers, which are an important component for achieving the overall power transfer efficiency (PTE), have been carried out [16], [18]. Previous research and experiments on MPT have proved that MPT can operate with high efficiency, even approaching 100%. However, such an MPT system would be too large to apply to practical mobile applications in our daily lives. Although the optimal transmitting field has been found previously, it was derived using an ideal receiving aperture whose shape is circular or rectangular with a symmetric tangential field distribution. Hence, the results cannot be applied to practical mobile antennas [5]–[11].

Moreover, several methods were proposed for an efficient WPT via the radiative field in small-scale scenarios: retro-directive array (RDA) and time-reversal (TR) techniques [19]–[26]. In [19], an RDA was used in a room scenario to transmit power wirelessly, where the efficiency was defined by the beam width. TR is a technique that flips the received signal in time to refocus the original field as an incoming wave [23], [24]. TR in the time domain can be interpreted as a phase conjugation in the frequency domain, especially for a monochromatic wave. Fink conducted many studies on electromagnetic (EM) TR using a cavity-like environment [23], [24]. TR is also used in open space using pulse waves to improve efficiency [25], [26]. However, most previous works on RDA and TR have provided little information about the efficiency bound of the WPT and the optimal shape of the transmitters within a given area.

In this communication, the PTE bound of the radiative WPT is derived for a given size of the transmitting area and the distance between the base station (BS) and the mobile antenna. Moreover, we propose a way to effectively minimize the transmitting area to achieve the target PTE, especially for practical mobile antennas. The proposed theory can be used for indoor WPT scenarios such as seminar rooms, where BS area minimization is an important factor relating to the cost, weight, and complexity of the system.

II. Theory

A. Power Transfer Efficiency

We first consider an arbitrary transmitting current as a BS surface at position A and a mobile antenna at position B, as shown in Fig. 1. We assume both electric and magnetic current flows in the tangential direction on the BS surface. Moreover, the mobile antenna is lossless and matched with its load impedance. The PTE is then defined as the receiving power at the load of the mobile antenna over the real input power at the transmitting current, i.e., $\eta = P_{B\_rec}/P_{A\_in}$, which is well known as the transducer gain. Our first goal is to determine the optimal transmitting current distribution for general types of mobile antennas.

Manuscript received January 24, 2019; revised April 30, 2019; accepted May 29, 2019. Date of publication June 18, 2019; date of current version August 12, 2019. This work was supported by the National Research Foundation of Korea (NRF) grant funded by the Korea government (MSIP) (no. 2016R1E1A1A01943375). *(Corresponding author: Sangwook Nam.)*

The authors are with the Institute of New Media Communication, School of Electrical and Computer Engineering, Seoul National University, Seoul 151-742, South Korea (e-mail: jhkim@ael.snu.ac.kr; snam@snu.ac.kr).

Color versions of one or more of the figures in this communication are available online at http://ieeexplore.ieee.org.

Digital Object Identifier 10.1109/TAP.2019.2922444

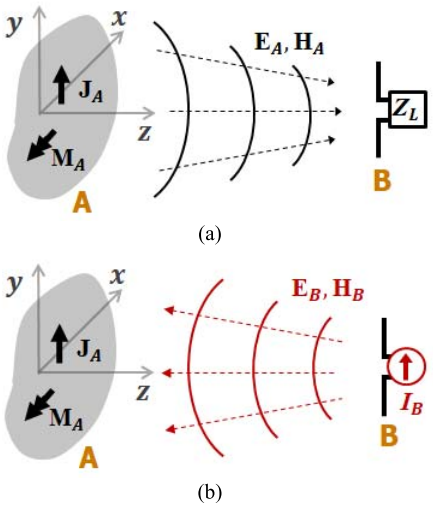

Fig. 1. Configurations for the analysis of radiative WPT. (a) Continuous base current ($\mathbf{J_A}$,$\mathbf{M_A}$) flowing on a surface emits a field ($\mathbf{E_A}$,$\mathbf{H_A}$) and a mobile antenna loaded with the impedance Z_L receives it. (b) Reciprocal situation: the mobile antenna with an exciting current source ($\mathrm{I_B}$) at the antenna port transmits propagating EM waves ($\mathbf{E_B}$,$\mathbf{H_B}$) when it operates in the transmitting mode.

As a first step to formulating the radiative WPT scenario, P_{A_in}, which denotes the real input power of the transmitting current, is presented in terms of the radiating EM field from the current at A, which is denoted as ($\mathbf{E_A}$,$\mathbf{H_A}$). Because we assume a lossless system, the real input power is equal to the radiating power propagating through the closed surface around A as follows:

$$P_{A\_in} = \frac{1}{4}\oint \left(\mathbf{E_A}\times\mathbf{H_A^*} + \mathbf{E_A^*}\times\mathbf{H_A}\right)\cdot\hat{\mathbf{n}}dS \tag{1}$$

where $\hat{\mathbf{n}}$ is the normal vector of the closed surface.

Because we discuss only the real radiating power, which consists of the propagating wave, the evanescent field is assumed to be negligible in this study. Therefore, the electric and magnetic fields radiated from the BS current can be related to the free space wave impedance Z_0.

The numerator of the PTE (P_{B_rec}) can be described in terms of the EM field and the current density. Using the open circuit voltage V_{B_oc} of the equivalent circuit model of the receiving mobile antenna, P_{rec_B} can be expressed as

$$P_{B\_rec} = \frac{|V_{B\_oc}|^2}{8R_L} \tag{2}$$

where R_L is the matched load resistance at the mobile antenna terminal, as shown in Fig. 1(a). The open circuit voltage V_{B_oc} is then represented as the radiating field from the current density on the BS surface and the source of the mobile antenna ($\mathbf{J_B}$, $\mathbf{M_B}$) using the following relation [27], [28]:

$$V_{B\_oc} = -\frac{1}{I_B}\int (\mathbf{E_A}\cdot\mathbf{J_B} - \mathbf{H_A}\cdot\mathbf{M_B})dS_B \tag{3}$$

where I_B is the magnitude of the current source at the mobile antenna when it is used as the transmitting antenna, as shown in Fig. 1(b).

However, it is too complicated to calculate $\mathbf{E_A}$ and $\mathbf{H_A}$, which are the radiated field from the current at A and include the scattered field by the conductor surface of the mobile antenna [27], [28]. Then we can use the reciprocity theorem to replace them using the field radiated by the mobile antenna ($\mathbf{E_B}$, $\mathbf{H_B}$), which is assumed to be known variables if the mobile antenna has been determined. The PTE is then expressed as follows:

$$\eta = \frac{1}{2R_L|I_B|^2}\frac{\left|\int (\mathbf{E_B}\cdot\mathbf{J_A} - \mathbf{H_B}\cdot\mathbf{M_A})\,dS_A\right|^2}{\oint \left(\mathbf{E_A}\times\mathbf{H_A^*} + \mathbf{E_A^*}\times\mathbf{H_A}\right)\cdot\hat{\mathbf{n}}dS}. \tag{4}$$

B. Optimal Transmitting Current

The analysis of PTE in (4) is tedious because it involves solving all the intricate integrals for the EM field vectors from the BS current at A ($\mathbf{E_A}$, $\mathbf{H_A}$), as described in previous studies [5]–[11]. Here, we use a simple idea to determine the denominator of (4) for the ease of calculation.

Let us consider two independent scenarios in which the BS current at A and the mobile antenna at B radiate, as shown in Fig. 1(a) and (b). Because the input power of the two cases can be expressed as radiating power, which is a real value, they can be related to an arbitrary positive real constant value α, i.e., $P_{in\_A} = \alpha \times P_{in\_B}$. Therefore, the denominator of (4) can be represented in terms of ($\mathbf{E_B}$, $\mathbf{H_B}$), the radiating field from the mobile antenna at B, with the scaling constant α, so that the optimization problem for the PTE can be easily solved without complex calculations.

The PTE is clearly formulated using the following matrix forms of the field and current density vectors:

$$\psi = \begin{pmatrix}\mathbf{E}\\ \mathbf{H}\end{pmatrix} \tag{5a}$$

$$\rho = \begin{pmatrix}\mathbf{J}\\ -\mathbf{M}\end{pmatrix}. \tag{5b}$$

Replacing the real input power of the mobile antenna at B, (4) becomes

$$\eta = \frac{1}{\alpha}\frac{\left|\langle\psi_B^T, \rho_A^\dagger\rangle_{S_A}\right|^2}{\left|\langle\psi_B^T Z, \psi_B^T\rangle_S\right|^2} \tag{6}$$

where $\langle f, g\rangle_S$ denotes the inner product of function f and the conjugate of function g on the given surface (i.e.,$\int fg^*dS$), ψ_B^T is the transpose of the matrix representing the fields radiated by the mobile antenna at B [Fig. 1(b)], and $\rho_A^\dagger$ is the Hermitian of the current distribution on the BS surface at A. Matrix Z represents the relationship between the electric field and the magnetic field radiated by the mobile antenna, as described in (7). Because only the pointing vector normal to the BS surfaces is considered, as described in (4), matrix Z can be expressed in terms of the inner product of the radial vector of the propagating fields (ψ_B) and the normal vector of the BS surface (S_A), i.e., $\hat{\mathbf{r}}\cdot\hat{\mathbf{n}}$. This indicates the wave impedance of the mobile fields in the direction normal to the BS surface currents, which is expressed as follows:

$$Z = \begin{pmatrix}(\hat{\mathbf{r}}\cdot\hat{\mathbf{n}})/Z_0 & 0\\ 0 & (\hat{\mathbf{r}}\cdot\hat{\mathbf{n}})\,Z_0\end{pmatrix}. \tag{7}$$

The expression in (6) is a well-known form used in optimization problems for estimation and detection [29], [30]. Because matrix Z is positive definite, there exists a nonsingular matrix U such that $Z = UU^\dagger$. The maximum value of (6) can be obtained using the Cauchy–Schwarz inequality. The resultant optimum transmitting base current on the surfaces is $\rho_{A\_opt} = k(\psi_B^T Z)^\dagger$, which is

$$\mathbf{J_{A\_opt}} = k\frac{1}{Z_0}(\hat{\mathbf{r}}\cdot\hat{\mathbf{n}})\mathbf{E_B^*} \tag{8a}$$

$$\mathbf{M_{A\_opt}} = -kZ_0(\hat{\mathbf{r}}\cdot\hat{\mathbf{n}})\mathbf{H_B^*} \tag{8b}$$

where k is a proportional constant. The value of k can be determined using the initial assumption $P_{in\_A} = \alpha \times P_{in\_B}$. The impressed input power at the source A is

$$P_{in\_A}=\frac{1}{4}Re\left(\int \mathbf{E_A}\cdot\mathbf{J_A^*}+\mathbf{H_A^*}\cdot\mathbf{M_A}dS_A\right). \quad (9)$$

The radiating field ψ_A in (9) can be expressed in terms of source current ρ_A using the equivalent theorem. Applying the optimal currents of (8) to the impressed power of (9) to solve the initial condition, the square of the proportional constant is given by

$$k^2=\alpha\frac{\langle\psi_B^T Z,\psi_B^T\rangle_S}{\langle\psi_B^T Z,\psi_B^T\rangle_{S_A}}. \quad (10)$$

As a result, optimal efficiency becomes

$$\eta_{opt}=\frac{|\langle\psi_B^T Z,\psi_B^T\rangle_{S_A}|}{|\langle\psi_B^T Z,\psi_B^T\rangle_S|}. \quad (11)$$

We note that the denominator of (11) indicates the power radiated by the mobile antenna at B, while the numerator implies the power passing through the region of the given BS surface at A (S_A). Therefore, the optimal efficiency can be understood in terms of the radiating field for the mobile antenna and the shape of the BS surface.

We can see that the optimum current on the BS surface for the mobile antenna in (8) is related to the conjugation of the tangential fields, which are radiated from the mobile antenna in the transmitting mode [Fig. 1(b)]. Note that the optimum current is the same as the TR current in the time-harmonic case when the scaling factor α is 1 and the propagating vector is aligned with the normal vector ($\hat{\mathbf{r}}\cdot\hat{\mathbf{n}}=1$) [23]–[25]. This implies that the maximum PTE can be obtained when the radiating field ($\mathbf{E_B},\mathbf{H_B}$) of the mobile antenna in the transmitting mode is reconstructed in the reverse (inward) propagating direction. Therefore, the correlation between the transmitting field from the BS and the radiating field of the mobile antenna is an important factor that determines the PTE.

Note that the proposed theory can be applied to general receiving antennas to reveal the shape of the optimum transmitting current and the efficiency bounds, while previous works have generally used symmetric receiving apertures.

C. Minimum Transmitting Area

Following the results of the previous section, the optimum BS current should flow on the whole of the surface through which the radiating field of the mobile antenna passes to achieve 100% PTE. However, it is impossible to use the entire area as a transmitting BS from a practical point of view. Therefore, we must determine the optimal shape of the BS current that minimizes the transmitting area, as well as the PTE bound when using the allowable area.

The derivation of (11) and its results are valid not only for a closed surface of BS but also for an arbitrary unclosed surface. If the denominator in (11) is fixed, the numerator then becomes the factor determining the PTE. Following the terms in (4) with (8), V_{B_oc}, which is a critical factor determining the PTE, is defined as the correlation of the field emitted from the mobile ψ_B and the optimal source ρ_{A_opt} on the surface of the BS [Fig. 1(b)]. Therefore, in order to maximize the PTE and use the minimum area of the transmitting surface, it is necessary to use the region with high current flow. To maximize the integral of the numerator over a limited transmitting area, any base current below a certain value should be removed because it contributes less to the receiving power of the mobile antenna. Using this approach, the maximum PTE and the minimum transmission area can be related.

For the sake of better understanding, the flow chart in Fig. 2 explains the method used to maximize the PTE by decreasing the transmitting area. The process is based on the arrangement of the BS and the mobile antenna, the radiating fields of the mobile antenna, and the results of the proposed theory in (8) and (11). The proper use of the "cut" value can link each parameter.

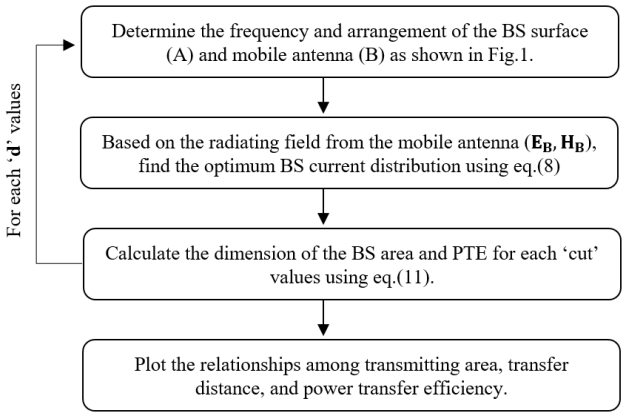

Fig. 2. Flowchart of the relationships among the transmitting area, transfer distance, and the PTE.

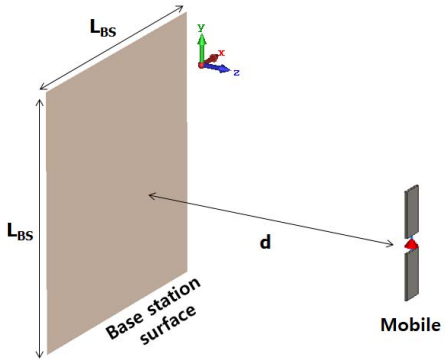

Fig. 3. Configuration for the numerical examples. The BS surface on which the ideal electric and magnetic currents flow on the xy plane with a size of $L_{BS}\times L_{BS}$. The mobile antenna, which can be any type of practical antenna, is placed at a distance d from the BS surface.

III. Numerical Examples

The proposed theory is then used to analyze three kinds of actual antennas. A 0.5λ dipole and patch antenna are used as representative examples of mobile antennas, and a high-gain horn antenna is described as a reference for an aperture antenna. Fig. 3 shows the configuration of the mobile antenna and the transmitting BS surface which could also be a spatially distributed or conformal surface. The transmitting current is assumed to be an ideal electric and magnetic current flowing on the tangential surface of the BS area. The size of the transmitting surface is $L_{BS}\times L_{BS}$. The BS and the mobile antennas are separated by the transfer distance d. The resonance frequency of the mobile antenna is set to 2.4 GHz (the licensed ISM band), but can be scaled arbitrarily for specific applications. The value of d is set to 0.7 m (5.6λ), and that of L_{BS} is set to 8 m (64λ) to observe the shape of the optimal current in the radiative near-field region.

A. Dipole Antenna

The first example of a mobile antenna considered in this study is a commonly used 0.5λ dipole that is aligned in the y-direction. The proposed theory is applied to determine the minimum transmitting

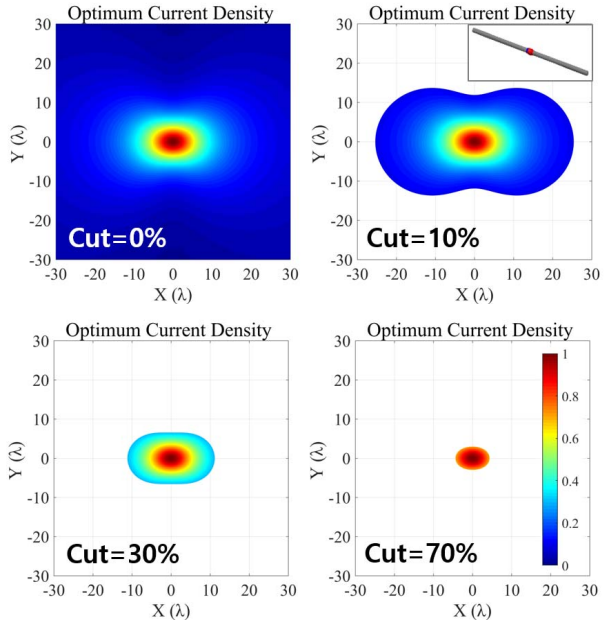

Fig. 4. Magnitude of the optimal current density on the BS surface when a 0.5λ dipole is used as a mobile antenna. The current density below a certain value (cut) is removed to minimize the transmitting area. The shape of the optimal transmitting current varies from a jar shape to an elliptical shape.

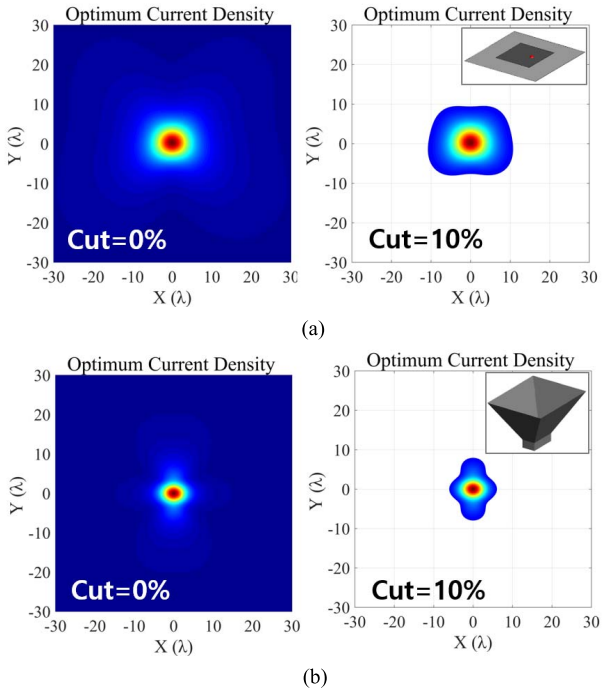

Fig. 5. Normalized magnitude of the optimal current density for unidirectional antennas. (a) Results of a patch antenna with a gain of 9.4 dBi and (b) results of a horn antenna with a gain of 14.8 dBi. Both results show much smaller optimal regions than the dipole antenna does for a cut value of 10%.

area and the efficiency bound of the dipole antenna. The normalized optimal current distribution for the mobile antenna is plotted in Fig. 4. The current on the transmitting surface is removed according to a certain percentage (called the "cut") of the maximum value of the square root of the normal pointing vector, as shown in Fig. 4. When the cut value is 0%, the entire current on the given transmitting surface is used. The results show that the shape of the optimal transmitting current distribution is not a circle or rectangle, but varies from a jar shape to an oval shape according to either the target efficiency or available transmitting area, which are both related to the cut value. Applying this approach, the target PTE can be obtained using a minimized transmitting area or a smaller number of transmitting antennas.

As an example, the transmitting area for a cut of 10% is about $1185\lambda^2$ (18.5 m^2) and the maximum PTE is about 40.5%. When the cut value is 30%, the area of the transmitting surface is about $250\lambda^2$ (3.9 m^2) and the optimal efficiency is about 29.5%. However, the ability to reproduce an omnidirectional field using only one side of a planar transmitting surface is limited. Because the dipole emits an omnidirectional EM field, the BS also needs to reconstruct the radiating field of the dipole antenna in a reverse way. Therefore, the PTE for a dipole antenna is inevitably low.

B. Patch Antenna

To improve the PTE using a single planar transmitting BS surface, a unidirectional patch antenna is designed. The patch antenna is placed on the *xy* plane facing the BS surface. The lengths of the square patch and the square ground plane are about 0.5λ and 1λ, respectively. The direct feed is used with an offset in the *y*-direction resulting in the *y*-polarized radiating field with a gain of 9.4 dBi. The magnitude of the optimal current density is shown in Fig. 5(a). Because the designed patch antenna radiates an asymmetric field caused by the diffraction effect of the compact ground plane, the magnitude of the optimal current density is slightly squashed. Compared with the optimal transmitting current of the dipole antenna, the current is concentrated in a smaller region. For a cut value of 10%, the size of the remaining BS area is about $330\lambda^2$ (5.2 m^2) and the maximum PTE is about 85.0%, which is much higher than that of the dipole antenna.

C. Horn Antenna

A horn antenna is employed to demonstrate the proposed method for a realistic aperture antenna and compare its PTE with the ideal receiving apertures reported in the preceding works. The operating frequency is also set to 2.4 GHz, and the width of the square horn aperture is 1.9λ. The radiating aperture of the horn antenna is placed in the center of the *xy* plane at a distance of d from the BS surface, emitting a *y*-polarized field with a gain of 14.8 dBi. Fig. 5(b) shows the optimal transmitting current for the horn antenna. As shown in Fig. 5(b), it can focus more of the field on the smaller BS surface. When a cut value of 10% is applied, the existing BS area is only $121\lambda^2$ (1.9 m^2), whereas the maximum efficiency is 90.1%.

IV. Results and Discussion

Using the optimum current distribution and the minimum transmitting area, the maximum PTE bounds relative to the size of the transmitting surface and the transfer distance are investigated. The efficiency bounds for the three types of mobile antennas are shown in Fig. 6(a). The transmitting current on the BS surface outside $L_{BS} \times L_{BS}$ ($L_{BS} = 64\lambda$) is not considered, because it is negligible. The maximum PTE bound for the dipole antenna, denoted as a black line, is relatively low (44.2%) compared with those of the other cases. Because the dipole antenna has an omnidirectional radiation pattern, the maximum PTE cannot exceed 50% when using only one planar transmitting surface. However, if the BS surface was implemented on both sides of the dipole or as a conformal shape, the maximum efficiency bound would be increased. To compare the size of the

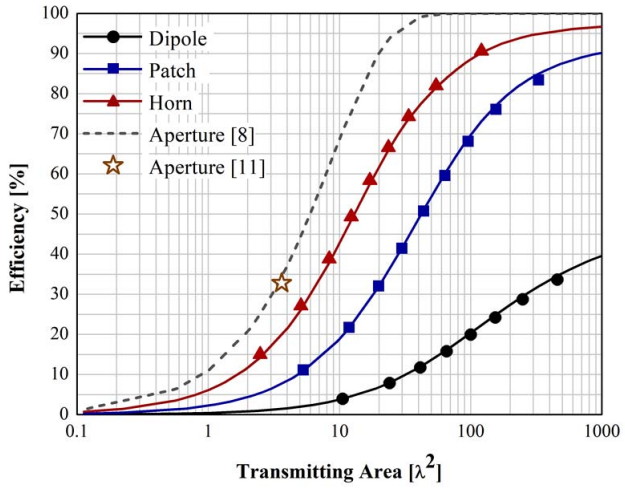

(a)

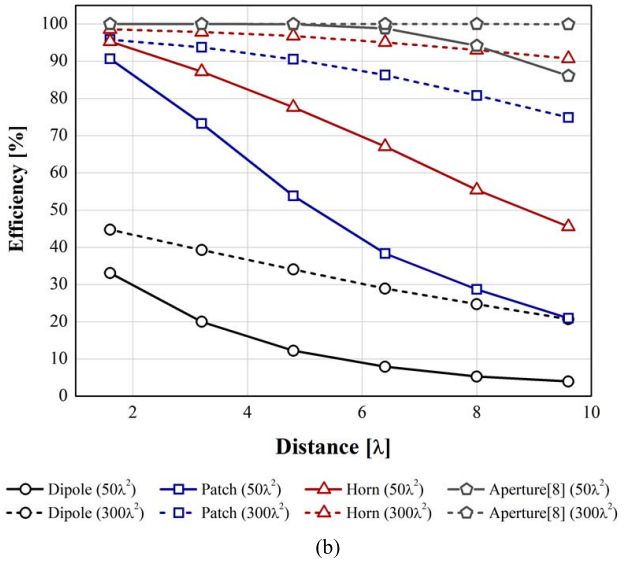

(b)

Fig. 6. Comparison of the PTE bounds of the mobile antennas with operating frequencies of 2.4 GHz ($\lambda = 0.125$ m). The aperture dimension of the horn antenna is identical to the ideal apertures for PTE comparison with data reported in [8] and [11]. (a) Efficiency bound according to the size of the transmitting area. The lines indicate the theoretical efficiency bound, whereas the solid symbols are simulated values. (b) Efficiency bounds in terms of the distance between the BS surface and the mobile antenna. The solid and dashed lines indicate transmitting areas of $50\lambda^2$ and $300\lambda^2$, respectively. The hollow symbols indicate the calculated points.

source area of each antenna, we consider a target PTE of 20%. As shown in Fig. 6(a), a transmitting area of $100\lambda^2$ (1.57 m^2) would be required to achieve this PTE using a dipole antenna.

In contrast, the PTE result of the patch antenna is highly improved. This is because the patch emits most of its field to a single side, which focuses the radiating field better on the BS surface. For the patch antenna, the PTE of 20% can be achieved by using a transmitting area of $11\lambda^2$ (0.17 m^2). If the patch antenna is designed to focus more of the field on the BS surface, the PTE can be further increased, although the area of the transmitting surface would be the same.

A horn antenna, which is a type of aperture antenna, yields the best performance. The PTE bound of the horn antenna converges to nearly 97.4% for large size of the transmitting aperture. When the horn antenna is used, a transmitting area of only $4\lambda^2$ (0.06 m^2) can attain the target PTE.

The PTE bounds reported previously in [8] and [11] are compared with the results obtained by the proposed method in Fig. 6. The PTE bound results cannot be compared exactly because the definition of the receiving power differs among the previous and current works. For an approximate comparison, a horn antenna is employed as a representative practical aperture antenna with the same size of the ideal receiving apertures used in [8] and [11]. The results in Fig. 6(a) show the certain difference in PTE bounds among them, describing the superior performance of the previous works. This difference arises from [5] to [11] defining the receiving power as the power passing through the ideal receiving aperture in which the tangential field is focused as the waist of the Gaussian beam. However, we used the real receiving power at the load of the mobile antennas, which is a more realistic definition because the practical mobile antenna is hard to capture all of the through power. Therefore, the efficiency bounds from the previous methods are unsuitable for mobile antennas, while the proposed theory can provide the practical maximum efficiency bound and the shape of the optimal transmitting area. Notably, the proposed theory can also be applied to a general transmitting BS surface shape, e.g., the top and bottom surfaces of a rectangular room or a conformal shape. In contrast, previous methods have assumed that the receiving aperture was unidirectional or even symmetric.

Here, the PTE data reported in [11] are compared to those obtained in this study only at one point, as shown in Fig. 6. This is because [11] used the assumption that the transmitting aperture and receiving aperture were identical in size, which was also symmetric. Therefore, the PTE bounds in various configurations could not be compared.

Note that the PTE of radiative WPT is not a function of the operating frequency when all of the electrical lengths of the system are fixed. This is because the magnitude of the optimum base current on the given tangential surface is determined solely by the radiating field pattern of the mobile antenna, as described in (8). It can also be explained by (11) with the configuration of Fig. 1(b). Equation (11) implies that the maximum PTE is the ratio of the power radiated to the entire space to the power passing through the given BS surface. However, it should be noted that when the transfer distance (d) is fixed in the meter for a specific WPT scenario, the electrical distance is changed, and thereof the efficiency bounds are modified.

To confirm the validity of the proposed theory, a full wave EM simulator called FEKO was used. Because the simulation of a continuous current sheet using full-wave EM tools is not available, numerous infinitesimal electric and magnetic dipoles were used to emulate the continuous base current sheet [31], [32]. The distance between each infinitesimal dipole was 0.33λ in the x- and y-directions. The operating frequency was set to 2.4 GHz. The simulation PTE results are defined as the ratio of the receiving power at the matched load of the mobile antenna to the total input power of the numerous infinitesimal sources. The discrete simulation points are plotted in Fig. 6(a) using solid symbols. The maximum relative errors are 2.8%, 1.4%, and 0.5% for the dipole, patch, and horn antenna, respectively. These differences occur because the discrete infinitesimal dipoles cannot realize an exact optimum base current, which is continuous. The theoretical and simulated maximum PTE results are in good agreement, confirming the proposed theoretical efficiency bound for a given area.

Fig. 6(b) shows the efficiency bound of the ideal aperture and the three types of antennas in terms of the distance between the BS surface and the mobile antennas. The solid and dashed lines indicate the cases with the transmitting areas of $50\lambda^2$ and $300\lambda^2$, respectively. The hollow symbols indicate the calculated points in terms of the transfer distance. The gray lines represent the data for the previous study in [8] and show a higher PTE than the real antennas. The graph shows that the patch antenna shows a better performance than the dipole antenna, although the efficiency of the patch antenna declines rapidly with distance. It also shows that MPT can achieve

high efficiency (up to 89%) even with a transmitting area of only $50\lambda^2$ (0.78 m^2) and a compact mobile patch antenna located in the radiative near-field region.

V. Conclusion

In this study, for MPT, the bound of the PTE and the optimal shape of the transmitting surface were proposed using simplified analytical steps that can also be applied to the general types of mobile antennas. It was shown that the phase conjugation of the mobile field is the optimum transmitting current on the BS surface. Note that the radiation characteristics of a mobile antenna that can concentrate the field on the BS surface are important factors in determining the maximum PTE bound. Following the results, clear differences among the PTE bounds are found for identical sized ideal apertures in the previous works and a practical horn antenna in the current work. Therefore, the proposed theory can provide analytical and physical insights for radiative WPT using practical mobile antennas, which cannot be understood based on previous research. On the other hand, the results show that MPT using a compact mobile antenna, such as a patch antenna, can achieve high PTE when the transfer distance is within the Fresnel region. It is expected that the basic knowledge of this study can assist research on MPT, especially for practical mobile applications in daily life.

References

[1] W. C. Brown, "Adapting microwave techniques to help solve future energy problems," *IEEE Trans. Microw. Theory Techn.*, vol. MTT-21, no. 12, pp. 753–763, Dec. 1973.

[2] W. C. Brown, "The history of power transmission by radio waves," *IEEE Trans. Microw. Theory Techn.*, vol. MTT-32, no. 9, pp. 1230–1242, Sep. 1984.

[3] W. C. Brown, "Experiments involving a microwave beam to power and position a helicopter," *IEEE Trans. Aerosp. Electron. Syst.*, vol. AES-5, no. 5, pp. 692–702, Sep. 1969.

[4] P. E. Glaser, "Power from the sun: Its future," *Science*, vol. 162, no. 3856, pp. 857–861, 1968.

[5] G. Goubau and F. Schwering, "On the guided propagation of electromagnetic wave beams," *IRE Trans. Antennas Propag.*, vol. 9, no. 3, pp. 248–256, May 1961.

[6] G. Goubau and P. Schwering, "Free space beam transmission," in *Microwave Power Engineering*, vol. 1, C. Okress, Ed. New York, NY, USA: Academic, 1968, pp. 241–255.

[7] G. Goubau, "Microwawe power transmission from an orbiting solar power station," *J. Microw. Power*, vol. 5, no. 4, pp. 223–231, 1970.

[8] N. Shinohara, "Power without wires," *IEEE Microw. Mag.*, vol. 12, no. 7, pp. S64–S73, Dec. 2011.

[9] N. Shinohara, *Wireless Power Transfer Via Radiowaves*. Hoboken, NJ, USA: Wiley, 2014.

[10] A. Kay, "Near-field gain of aperture antennas," *IRE Trans. Antennas Propag.*, vol. 8, no. 6, pp. 586–593, Nov. 1960.

[11] G. Borgiotti, "Maximum power transfer between two planar apertures in the Fresnel zone," *IEEE Trans. Antennas Propag.*, vol. AP-14, no. 2, pp. 158–163, Mar. 1966.

[12] H. Matsumoto, "Research on solar power satellites and microwave power transmission in Japan," *IEEE Microw. Mag.*, vol. 3, no. 4, pp. 36–45, Dec. 2002.

[13] N. Shinohara, "Beam control technologies with a high-efficiency phased array for microwave power transmission in Japan," *Proc. IEEE*, vol. 101, no. 6, pp. 1448–1463, Jun. 2013.

[14] S. Sasaki, K. Tanaka, and K.-I. Maki, "Microwave power transmission technologies for solar power satellites," *Proc. IEEE*, vol. 101, no. 6, pp. 1438–1447, Jun. 2013.

[15] J. J. Schlesak, A. Alden, and T. Ohno, "A microwave powered high altitude platform," in *IEEE MTT-S Int. Microw. Symp. Dig.*, New York, NY, USA, May 1988, pp. 283–286.

[16] N. Shinohara and H. Matsumoto, "Experimental study of large rectenna array for microwave energy transmission," *IEEE Trans. Microw. Theory Techn.*, vol. 46, no. 3, pp. 261–268, Mar. 1998.

[17] N. Shinohara, H. Matsumoto, and K. Hashimoto, "Phase-controlled magnetron development for SPORTS: Space power radio transmission system," *URSI Radio Sci. Bull.*, vol. 310, no. 310, pp. 29–35, Sep. 2004.

[18] C. Wang, N. Shinohara, and T. Mitani, "Study on 5.8-GHz single-stage charge pump rectifier for internal wireless system of satellite," *IEEE Trans. Microw. Theory Techn.*, vol. 65, no. 4, pp. 1058–1065, Apr. 2017.

[19] Y. Li and V. Jandhyala, "Design of retrodirective antenna arrays for short-range wireless power transmission," *IEEE Trans. Antennas Propag.*, vol. 60, no. 1, pp. 206–211, Jan. 2012.

[20] M. Ettorre, W. A. Alomar, and A. Grbic, "Radiative wireless power-transfer system using wideband, wide-angle slot arrays," *IEEE Trans. Antennas Propag.*, vol. 65, no. 6, pp. 2975–2982, Jun. 2017.

[21] M. Ettorre, W. A. Alomar, and A. Grbic, "2-D Van Atta array of wideband, wideangle slots for radiative wireless power transfer systems," *IEEE Trans. Antennas Propag.*, vol. 66, no. 9, pp. 4577–4585, Sep. 2018.

[22] Z. Nie and Y. Yang, "A model independent scheme of adaptive focusing for wireless powering to in-body shifting medical device," *IEEE Trans. Antennas Propag.*, vol. 66, no. 3, pp. 1497–1506, Mar. 2018.

[23] G. Lerosey, J. de Rosny, A. Tourin, A. Derode, G. Montaldo, and M. Fink, "Time reversal of electromagnetic waves," *Phys. Rev. Lett.*, vol. 92, no. 19, May 2004, Art. no. 193904.

[24] J. de Rosny, G. Lerosey, and M. Fink, "Theory of electromagnetic time-reversal mirrors," *IEEE Trans. Antennas Propag.*, vol. 58, no. 10, pp. 3139–3149, Oct. 2010.

[25] R. Ibrahim *et al.*, "Experiments of time-reversed pulse waves for wireless power transmission in an indoor environment," *IEEE Trans. Microw. Theory Techn.*, vol. 64, no. 7, pp. 2159–2170, Jul. 2016.

[26] R. Ibrahim *et al.*, "Novel design for a rectenna to collect pulse waves at 2.4 GHz," *IEEE Trans. Microw. Theory Techn.*, vol. 66, no. 1, pp. 357–365, Jan. 2018.

[27] V. H. Rumsey, "Reaction concept in electromagnetic theory," *Phys. Rev.*, vol. 94, no. 6, pp. 1483–1491, Jun. 1954.

[28] R. F. Harrington, *Time-Harmonic Electromagnetic Fields*. Piscataway, NJ, USA: IEEE Press, 2001.

[29] H. Cox, R. Zeskind, and M. Owen, "Robust adaptive beamforming," *IEEE Trans. Acoust., Speech, Signal Process.*, vol. ASSP-35, no. 10, pp. 1365–1376, Oct. 1987.

[30] J. M. Steele, *The Cauchy-Schwarz Master Class*. New York, NY, USA: Cambridge Univ. Press, 2004.

[31] S. M. Mikki and A. A. Kishk, "Theory and applications of infinitesimal dipole models for computational electromagnetics," *IEEE Trans. Antennas Propag.*, vol. 55, no. 5, pp. 1325–1337, May 2007.

[32] S. Clauzier, S. M. Mikki, and Y. M. M. Antar, "Design of near-field synthesis arrays through global optimization," *IEEE Trans. Antennas Propag.*, vol. 63, no. 1, pp. 151–165, Jan. 2015.